Dorsal striatal dopamine induces fronto-cortical hypoactivity and implies reduced anxiety and compulsive behaviors in rats

Authors: Agata Casado-Sainz[1]†, Frederik Gudmundsen[1]†, Simone L. Baerentzen[1], Denise Lange[2], Annemette Ringsted[1], Isabel Martinez-Tajada[1], Siria Medina[1], Hedok Lee[3], Claus Svarer[1], Sune H. Keller[4], Martin Schain[1], Celia Kjaerby[5], Patrick M. Fisher[1], Paul Cumming[6,7], Mikael Palner[1,8,9]*

Agata.Casado@nru.dk, frederik.gudmundsen@nru.dk, slb@clin.au.dk, Denise.Lange@dlr.de, annemetteringsted@gmail.com, imate@elektro.dtu.dk, siriamedinaa@gmail.com, hedoklee@gmail.com, Claus.Svarer@nru.dk, Sune.Hoegild.Keller@regionh.dk, Martin.Schain@nru.dk, celia.kjaerby@sund.ku.dk, patrick.fisher@nru.dk, paul.k.cumming@gmail.com, mikael.palner@nru.dk

Affiliations:

[1] Neurobiology Research Unit, Copenhagen University Hospital, Copenhagen, Denmark

[2] Institute of Aerospace Medicine, German Aerospace Center (DLR), Cologne, Germany.

[3] Department of Anesthesiology and Pediatric Anesthesiology, Yale University, New Haven, CT, United States

[4] Department of Clinical Physiology, Nuclear Medicine and PET, Copenhagen University Hospital, Copenhagen, Denmark

[5] Center for Translational Neuromedicine, University of Copenhagen, Copenhagen, Denmark

[6] Department of Nuclear Medicine, Inselspital, Bern University, Bern, Switzerland

[7] School of Psychology and Counselling, Queensland University of Technology, Brisbane, Australia

[8] Clinical Physiology and Nuclear Medicine, Department of Clinical Research, University of Southern Denmark, Odense, Denmark

[9] Department of Nuclear Medicine, Odense University Hospital, Odense, Denmark

† These authors contributed equally to the publication
* Corresponding author, mikael.palner@nru.dk
Neurobiology Research Unit
6-8 Inge Lehmanns Vej
Rigshospitalet, build. 8057
DK-2100 Copenhagen, Denmark
Phone: +45 9399 6712

1 **One Sentence Summary:** Dorsal striatum dopamine induce fronto-cortical hypoactivity and
2 reduce compulsive behaviors in rats
3
4 **Abstract:**

5 Dorsal striatal dopamine transmission engages the cortico-striato-thalamo-cortical (CSTC) circuit,
6 which is implicated in many neuropsychiatric diseases, including obsessive-compulsive disorder
7 (OCD). Yet it is unknown if dorsal striatal dopamine hyperactivity is the cause or consequence of
8 changes elsewhere in the CSTC circuit. Classical pharmacological and neurotoxic manipulations
9 of the CSTC and other brain circuits suffer from various drawbacks related to off-target effects
10 and adaptive changes. Chemogenetics, on the other hand, enables a highly selective targeting of
11 specific neuronal populations within a given circuit. In this study, we developed a chemogenetic
12 method for selective activation of dopamine neurons in the substantia nigra, which innervating the
13 rat dorsal striatum. We used this model to investigate effects of targeted dopamine activation on
14 CSTC circuit function, especially in fronto-cortical regions. We found that chemogenetic
15 activation of these neurons increased movement, as expected from dopamine release, rearings and
16 time spend in center, while it also lowered self-grooming and increased prepulse inhibition in
17 females. Remarkably, we observed reduced [^{18}F]FDG metabolism in frontal cortex, following
18 dopamine activation in the dorsal striatum, yet total glutamate levels- in this region were increased.
19 A finding which may help explain the contradiction in some clinical studies of increased [^{18}F]FDG
20 metabolism and lower glutamate levels in diseases like OCD. Taken together, these results
21 establish the importance of nigro-striatal dopamine transmission for modulating CSTC function,
22 especially with respect to fronto-cortical activity, glutamate levels and behaviors related anxiety
23 and compulsive actions.
24
25

2

Introduction

Real progress in the development of therapeutic approaches for a range of neuropsychiatric disorder has been stalled for years. One reason is likely due to the lack of causal whole brain analysis of functional circuits, which are usually done for one region or projection at the time. We set out to discover how manipulation of one dopaminergic projection affects changes throughout the cortico-striato-thalamo-cortical (CSTC) circuit using *in vivo* whole-brain imaging and chemogenetics.

The CSTC circuit relays cortical activity, through the striatum, midbrain and thalamus back to the cortex. Cortical pyramidal neurons project to the dorsal striatum, where spiny projection neurons (SPN) then subserve an integration of direct (go) or indirect (no-go) output pathways that relay signals to the thalamus via the substantia nigra pars reticulata (SNr). The thalamus then communicates the processed signal back to frontal cortex to complete the circuit [2,6]. The activity of the CSTC circuit is modulated by nigro-striatal dopamine projections to the dorsal striatum. Changes in striatal dopaminergic activity have been linked to perturbations of cognitive functions in multiple neuropsychiatric or neurodegenerative diseases [1] such as obsessive compulsive disorder (OCD) [2] and schizophrenia [3]. While showing distinct phenomenologies, these conditions have overlapping behavioral phenotypes, including obsessions, compulsions, and sensory gating deficits, which are linked to altered dopaminergic transmission within the striatum [4,5].

Molecular imaging studies by positron emission tomography (PET) in people with OCD have shown changes in striatal dopamine receptor availability [5], metabolic hyperactivity especially in the orbito-frontal cortex (OFC), and increased metabolic connectivity from frontal cortex to the caudate [7–10], which is the equivalent of the medial dorsal striatum (mDS) in rodents [11]. MR spectroscopy studies of such individuals have shown relatively reduced total glutamate+glutamine (Glx) and N-acetylaspartate levels in fronto-cortical regions [12–14]. These clinical imaging studies suggest the presence of a phenotype of abnormal CSTC circuit activity in OCD, although it is difficult to establish causal relationships based on clinical imaging without direct targeting of specific neuronal pathways. As such, it is unclear if altered striatal dopamine function is a driver for or rather a consequence of fronto-cortical dysfunction in neuropsychiatric disease.

Classical neurochemical approaches to modulate activity within the rodent CSTC include neurochemical lesions [15,16], and focal stereotaxic drug injections [17]. These chronic methods, in varying degrees, bring unintended perturbations or adaptive changes of the nervous system. Chemogenetics, on the other hand, enables a highly selective targeting of specific neuronal populations within a given circuit. In this study, we applied a selective retrograde chemogenetic transduction of the medial dorsal striatum (mDS) dopamine projections arising from the medial substantia nigra pars compacta (mSNpc). Using this model, we studied the effects of selective nigro-striatal dopamine activation on behavioral, and whole-brain CSTC circuit function in the

3

1   rodent brain. The combination of [^{18}F]FDG PET and MR Spectroscopy gives valuable knowledge
2   highly needed in order to interpret clinical neuroimaging findings in psychiatric disorders, and
3   suggest that the combination of these using PET/MR technology in patients may increase our
4   understanding of such disorders. We show that there is a causal relationship between increased
5   dorsal striatum dopamine and fronto-cortical hypoactivity, yet unexpectedly also an increase in
6   total glutamate levels. At the same time, dopamine activity in the dorsal striatum led to increased
7   locomotion, increase exploratory and anxiolytic effects, and a change in behavioral measures
8   related to CSTC circuit function and compulsive actions, lower self-grooming, lower startle
9   response and increased prepulse-inhibition of the startle response in females. These results in
10   otherwise behaviorally normal rats support the formulation of a novel hypothesis that potentiating
11   dopaminergic activity specifically in mDS will reduce anxiety and compulsive-like behavioral
12   symptoms which are related to hypercortical activity, like those present in disorders such as OCD.
13

14   **Materials and Methods**

15   *Animals*

16   Long Evans TH:Cre rats (LE Tg(TH:Cre 3.1)Deis) were purchased from the Rat Resource and
17   Research Center (RRRC, University of Missouri). This strain carries a transgene containing a Cre
18   recombinase inserted immediately before the start codon of the tyrosine hydroxylase gene (Witten
19   et al. 2011). Both male (♂ = ▲) and female (♀ = ▼) animal were used. Additional information of
20   breeding and ethics is located in the supplementary materials.

21   *Statistics*

22   Results are analyzed in GraphPad using a two-way ANOVA (behavioral experiments) or mixed
23   effects model (PET and MRS) analysis with repeated measure where appropriate with adjustment
24   for multiple comparisons. We report general effects of sex, treatment or vector injection with
25   significance (P) and degrees of freedom (F), while mixed effects models are noted with t-value
26   and DF. Individual group differences are noted only with respect to significance (P). Standard
27   deviations (SD) are reported throughout the results and figures. Significance is reported as ****
28     $P<0.0001$, *** $P<0.001$, ** $P<0.01$, * $P<0.05$.

29   *Retrograde chemogenetic transduction of dopaminergic projections in rats and mice*

30   Adult TH:Cre rats (250 g) rats were anesthetized with 3% isoflurane (vol/vol) in oxygen and placed
31   into a stereotactic frame (Kopf Instruments, Tujunga, CA, USA). Anesthesia was maintained with
32   1.5– 2% isoflurane; breathing, pain reflex, and body temperature was monitored throughout
33   surgery. The scalp was shaved and disinfected with successive swabs soaked in 70% iodine,
34   ethanol, and 0.1% lidocaine. An incision was then made down the midline of the scalp, the skull
35   was exposed, and burr holes were drilled above the target regions. The DREADD (mDS-
36   DREADD: AAV6-hSyn-DIO-mCherry-hM3D(Gq)-WPRE) (hM3Dq) and mCherry (mDS-

4

1   mCherry: AAV6-hSyn-DIO-mCherry-WPRE) carrying viral vectors (described in detail in the
2   supplementary materials) were injected bilaterally in the mDS at two locations in each hemisphere
3   (2 μL per location) (AP +1.1 mm, ML ± 2.5 mm, DV -5 mm and -6 mm), via a 10 μl Nanofil
4   syringe and 33GA beveled needle (World Precision Instruments, Sarasota, FL, USA) at an infusion
5   rate of 150 nL/min. After infusion, the needle was left in place for ten min to allow for diffusion
6   of the virus away from the needle tip before its slow withdrawal. Following injections, the scalp
7   was sutured and the rats were allowed to regain consciousness. Carprofen (5 mg/kg) was
8   administered subcutaneously as an analgesic before surgery and at 24 and 48 h after surgery.
9   Following surgery, rats were single-housed for one week, and their weight, fur, eyes and overall
10   movement were checked daily for signs of distress following the scheme of Roughan and Flecknell
11   [18]. Animals were then returned to group housing for two weeks prior to further experiments.

12   *Immunohistochemistry*

13   At the end of the experiments, rats were euthanized with an overdose of pentobarbital and
14   immediately perfused transcardially with 150-200 ml of ice-cold phosphate-buffered saline (PBS,
15   pH 7.4) followed by 100-150 ml of ice-cold 4% paraformaldehyde in PBS. Brains were removed
16   and stored in 4% paraformaldehyde for 24 h at 4 °C, rinsed twice with PBS, and then cryoprotected
17   in 30% sucrose/PBS. Brain sections 40 μm-thick obtained on a microtome were stored in
18   cryoprotectant solution at -20 °C. Free-floating sections were immunostained for mCherry (Cat.
19   #632543, TaKaRa Bio Europe) using the Avidin-Biotin Complex Peroxidase (ABC-P) method
20   and for TH (Cat. #P21962, Invitrogen) using fluorescent antibodies as described in detail in the
21   supplementary material.

22   *Locomotor activity and prepulse inhibition of the startle response*

23   First, we assessed the individual startle responses of the rats as described in detail in the
24   supplementary material. On the experimental day, locomotor activity and prepulse inhibition of
25   the startle response were recorded from 43 animals in cohort 1 at baseline and again after CNO
26   treatment (14 WT (7M / 7F), 15 mDS-DREADD (8M / 7F) and 14 mDS-mCherry rats (7M / 7F)).
27   Locomotor activity was assessed in a custom-made open field maze consisting of an 80 x 80 cm
28   arena enclosed by 65 cm opaque walls, with indirect, dim illumination (~10 Lux). On the test day,
29   rats received an i.p. injection of CNO (0.5 mg/kg in 5% DSMO/Saline), and 20 min later were
30   placed at the center of the open field and allowed to explore for 40 minutes. Behavior was recorded
31   with a Basler ace2 Pro video camera with a 4.5-12.5 mm F1.2 lens positioned directly above the
32   arena and analyzed using Ethovision software, with scoring of distance, velocity, center of field
33   entries, rearing and grooming. The arena was cleaned with soap and water and then dried between
34   each session. Immediately after the locomotion recordings, the rats were transferred to the startle
35   chamber for sensorimotor gating assessment, details of which are described in the supplementary
36   material.

5

1   *[^{18}F]FDG PET scanning*

2   The rats (n=14, (7 mDS-DREADD, 4F/3M), (7 mDS-mCherry, 4F/3M)) were fasted overnight
3   before the PET scan. At the day of the experiment, they received an s.c. injection of 0.5 mg/kg
4   CNO (0.5 mg/kg in 5% DSMO/Saline) or saline followed 20 min later by an i.p. injection of 14.1
5   ± 1.6 MBq FDG (from the clinical in-house production). The rats remained in their home cage for
6   45 minutes following the [^{18}F]FDG injection. Following this uptake period, the rats were sedated
7   with isoflurane (2–2.5% in oxygen) and placed in a homemade four rat insert in a Siemens HRRT
8   (High Resolution Research Tomograph) scanner [19] for a 45-min list-mode emission scan. The
9   rats were kept warm using an infrared lamp and monitored for respiration throughout the scan.
10   PET images were cropped to brain-only images for each rat and manually co-registration to an-
11   FDG-specific rat brain template. Individual scans were converted to SUV units and normalized to
12   whole-brain uptake as described in detail in the supplementary material. The images were averaged
13   per group/condition and the voxelwise difference was calculated between conditions. We
14   undertook a regional analysis for each animal in Nucleus Acumbens (NAc), mDS, lateral Dorsal
15   Striatum (lDS), Anterior Cingulate Cortex (ACC), mPFC, OFC, Thalamus (Thal), the midbrain
16   including ventral tegmental area and substantia nigra (MB), Hypothalamus (Hyp) and Cerebellum
17   (Cer), as described in detail in the supplementary material.

18   *Magnetic resonance spectroscopy*

19   All MR scans were performed on a Bruker BioSpec 94/30 USR MRI system (9.4T, 30 cm bore,
20   Bruker, Ettlingen, Germany) as previously described (29). In short, rats were anaesthetized with
21   2% isoflurane in oxygen, MRS was done sequentially in a 3 x 3 x 3 mm region in the right
22   hemispheric mDS and then in a 3 x 2 x 3 mm region in mPFC. The spectra were acquired using a
23   STEAM sequence with TE = 4 ms, TR = 4000 ms, 400 averages, eight dummy scans and 4096
24   points. VAPOR was used for water suppression. Metabolite concentration calculation was
25   performed by LCModel using water unsuppressed signal as an internal reference.
26
27   **Results**

28   *Selective chemogenetic targeting of nigro-striatal dopaminergic projections*
29   We first confirmed the retrograde transduction of nigrostriatal dopamine neurons. Injection of Cre-
30   dependent serotype 6 adeno associated viruses in the mDS of TH:Cre rats led to selective
31   retrograde expression of the mCherry reporter gene in dopamine projection neurons arising from
32   the mSNpc (Fig 1, A and B). Immunohistochemical identification of the mCherry reporter gene
33   showed excellent selectivity towards the target neurons. Two different viral vectors were injected
34   into the mDS, one carrying a Gq-coupled DREADD together with mCherry and the other only
35   mCherry (Figure 1D). The staining intensity and spread from the injection site confirmed a highly
36   reproducible target transduction in the mDS (Fig. S2A). There was no evident transduction of cell
37   bodies resident in the mDS, nor of non-TH:Cre positive cells in the mSNpc (Fig. 1, E-J). Notably,
38   the ventral tegmental area was devoid of mCherry-expressing somata (Fig. 1, E and I).

6

Nigro-striatal dopaminergic stimulation increases exploratory behaviors and lowers self-grooming

We then tested the efficacy of our transduction by locomotor activity. CNO significantly increased velocity in mDS-DREADD animals, with a maximal 90% increase occurring after 20 minutes of exploration, as compared with wildtype (WT) and mDS-mCherry animals (Fig. 2, A and B). The mDS-DREADD rats showed an increase in total distance travelled and total time spent in locomotion. WT rats had a 14% decrease in locomotion time following CNO treatment, which we attribute to a general habituation to the open field during the second exposure (Fig. 2E). Yet, the number of movement initiations (frequency) was similar in all groups (Fig. 2I). There was increased number of entries (+125%) and time spent (+119%) in the center of the open field for mDS-DREADD rats (P<0.0001, n=12) following CNO treatment (Fig. 2, F and J). Time spent rearing and number of rearing events were similarly increased by 66 and 99%, respectively (P<0.001, n=12) following CNO treatment in mDS-DREADD rats (Fig. 2, G and K). Self grooming time and bouts were likewise affected, but in the opposite direction, with significant reductions of -59% and -38%, respectively (P<0.001, n=12) following CNO treatment (Fig. 2, H and L). Similarly, for the second batch of animals used for the imaging experiments, there was a similar increase in total movement (P=0.003, n=9), center entries (P=0.005, n=9) and rearing (P=0.002, n=9) in mDS-DREADD animals following CNO treatment (Fig. S4, A-C). There were no main effects of transduction or sex on either behavior. Taken together, mDS-DREADD rats moved and explored more following CNO treatment compared to WT and mDS-mCherry rats, while spending less time self-grooming.

Nigro-striatal dopaminergic stimulation affects prepulse inhibition of the acoustic startle response differently in males and females

Prepulse inhibition (PPI) of the acoustic startle response is modulated by CSTC circuit function and impaired in related neuropsychiatric disorders like OCD [20–22]. To assess PPI, we first tested basal acoustic startle response (ASR) to different intensity sound pulses. The ASR was clearly measurable after exceeding 100 dB amplitude and plateaued at 110 dB both in males and females, with a maximal ASR (as measured at 120 dB) of $59.1 \pm 8.1\%$ in males (n=21) and $49.6 \pm 9.1\%$ in females (n=27) (Fig. 3A). We chose 110 dB as the pulse intensity for subsequent testing of pre-pulse inhibition (PPI). There was a sex difference in the ASR to various volumes of sound pulses (P<0.001, $F_{(1,46)}=25.2$), but no effect of transductions.

We then tested startle response (SR) to a 110 dB sound pulse with or without different intensity prepulses (all pulses are shown in Fig. S5A and D) and short-term habituation (STH) (Fig. S5B and E). There was no effect of transductions or treatment with CNO on the SR (Fig. 3, D and E), but there was an overall effect of sex. SR was greater in males ($58.1 \pm 3.8\%$, n=21) than in females ($48.6 \pm 4.3\%$, n=27) (P<0.001, $F_{(1,84)}=30.64$), as expected from the initial ASR test (Fig. 3A). There were no differences in mean STH between WT and transduction groups or between baseline

7

1   and CNO treatment. However, the mean STH was significant in all female groups combined (19.7
2   ± 6.2%; n=27) (Fig. S5B and E) (P=0.008, F(1,86)=7.3).

3

4   In general, SRs decreased in proportion to the amplitude of the prepulse, as expected (Fig. S5A
5   and D). There were no general effects of transduction or CNO treatment on SR in either sex. Yet,
6   a reduced SR following CNO treatment in mDS-DREADD females was just shy of statistical
7   significance (Ave. Diff. = 3.3 ± 1.5 %, p=0.0501 (F(1,9)=5.11)). We next assessed the latency
8   from startle pulse to startle onset and maximum peak of startle from the SR data above (Fig. S5C
9   and F). There were no differences in latency with prepulse only and no stimuli (Fig. S5H). Baseline
10   PPI following the 69 dB prepulse was higher in female than male rats (Fig. S5G) (P=0.006,
11   F(1,84)=7.86). Transduction did not affect baseline PPI (Fig. 3F and G, and Fig. S5G). There was
12   a general 24% increase in mDS-DREADD female rats for all pre-pulses amplitudes (P=0.022,
13   F(1,9)=7.6), and a 58% increase in female mDS-DREADD rats at the 69 dB prepulse condition
14   upon CNO treatment (Fig. 3G and I) (P=0.018, n=10).

15   *Nigro-striatal dopaminergic stimulation affects metabolic activity the medial prefrontal cortex and*
16   *orbitofrontal cortex.*

17   Next, we wanted to know how dorsal striatal dopamine effected clinical neuroimaging
18   measurements often used to study neuropsychiatric disorders. We used a whole-brain [^{18}F]FDG
19   PET approach to assess the glucose metabolism in the whole CSTC circuit at once. An image
20   analysis of voxel intensity showed a relative lower uptake of [^{18}F]FDG in cortical regions and
21   higher uptake in cerebellar regions in mDS-DREADD rats after CNO treatment (Figure 4A). On
22   a CSTC regional level, there were significant reductions in [^{18}F]FDG uptake in the mPFC (-9%,
23   P = 0.002, t = 4.06, DF = 60, N = 7) and OFC (-8%, P = 0.004, t = 3.73, DF = 49, N = 8) following
24   CNO treatment in mDS-DREADD rats. There were no effects on [^{18}F]FDG uptake in other CSTC
25   regions of mDS-DREADD, nor in mDS-mCherry rats (Fig. 4B), and no effects of sex or
26   transduction.

27

28   *Nigro-striatal dopaminergic stimulation increase glutamate and N-acetylaspartylglutamic acid*
29   *in medial prefrontal cortex and glutamate levels in dorsal striatum.*

30   Based on the [^{18}F]FDG PET findings (Fig. 4B), we chose two regions (mPFC and DS) for MR
31   spectroscopy (MRS) measurements of glutamate, glutamine, N-aspartate (NAA) and N-
32   acetylaspartylglutamic acid (NAAG) *in vivo.* There were significant increases in glutamate (P <
33   0.0001, t = 5.73, DF = 70), total NAA+NAAG (P = 0.006, t = 3.43, DF = 70) and total glutamate
34   + glutamine (P = 0.001, t = 3.95, DF = 70) levels in the mPFC following CNO treatment in mDS-
35   DREADD rats (Fig. 5, D and E). Furthermore, significant increases in glutamate (P < 0.0001, t =
36   5.67, DF = 70) and total glutamate + glutamine (P < 0.0001, t = 5.54, DF = 70) levels were found
37   in the mDS. We found no effect of sex in any group, nor for viral transductions in baseline
38   conditions. Contrary to our previous findings [23], CNO treatment in mDS-mCherry animals did

8

1   provoke significant reductions in glutamate ($P = 0.0002$, $t = 4.69$, $DF = 70$) and total glutamate +
2   glutamine ($P < 0.0001$, $t = 6.01$, $DF = 70$) levels (Fig. 6, F and G) in the mDS.
3
4   **Discussion**
5
6   We present a novel chemogenetic procedure for selective bilateral activation of nigro-striatal
7   dopamine projections innervating the rat mDS, which enabled us to test effects of dopaminergic
8   modulation of the CSTC circuit. In this animal model, we tested the specific hypothesis that
9   selective dopamine activation in the rat mDS would lower compulsive-related behaviors and
10   reduce cerebral metabolism in the frontal cortex. The least invasive, yet regional selective,
11   procedure for rodent studies may be chemogenetics, in which transduction of Designer Receptors
12   Exclusively Activated by Designer Drugs (DREADD) renders target neurons sensitive to G-
13   protein coupled activation/inactivation following injection of an exogenous ligand, such as
14   clozapine N-oxide (CNO) [24]. By enabling highly selective and reversible activation of specific
15   neuronal subtypes and pathways, chemogenetics presents a powerful approach for establishing
16   causal relationships.

17   *Nigro-striatal dopaminergic stimulation increases exploratory behaviors and lowers self-*
18   *grooming*

19   We targeted subdivisions of striatal dopaminergic innervations by using TH:Cre rats [25] treated
20   with retrograde neuronal transduction by the AAV6 serotype, as previously established in rats [26],
21   mice [27], and non-human primates [28]. We found that CNO increased lomomotor activity in all
22   mDS-DREADD rats. *In vivo* stimulation of hM3Dq DREADDs are well known to induce
23   phosphatidylinositol hydrolysis [24], c-fos activation [29–31], dopamine release [32], increased
24   dopamine neuron excitability with a burst firing pattern [30,31,33,34] and ultimately increased
25   locomotion as a behavioral read-out [30,35–39], which support our findings. We also observed an
26   increase in exploratory behaviors, entries into center field, and rearing in all mDS-DREADD rats
27   during chemogenetic activation. Such exploratory behaviors typically increase following treatment
28   with anxiolytic drugs [40,41], and decrease following stress [41,42], often in a manner independent
29   of hyperlocomotion, thus suggesting anxiolytic effects of the present perturbation of the CSTC
30   circuit.
31
32   Self-grooming is an innate rodent behaviour characterized by a sequential pattern of movements
33   [43], which serves as a useful proxy for compulsive behaviour [22,44,45]. Grooming time and
34   frequency are under control by the efferent activity of striatal SPNs. Whereas activation of D_1
35   receptors on SPNs of the direct ("go") pathway increase grooming, activation of D_2 receptors on
36   the indirect ("no-go") SPNs decrease grooming [43]. Our mDS-DREADD rats showed a
37   significant decrease of grooming frequency and duration during chemogenetic activation. This
38   may reflect preferential activation of the (D2-expressing) indirect pathway SPNs, although we
39   cannot rule out the possibility of secondary effect due to hyperlocomotion and increased

9

1 exploration. The preferential activation of the indirect pathway in our mDS-DREADD rats is
2 supported by a recent report that the dopamine fibres, which was mapped by retrograde tracing,
3 innervating the mDS predominantly target the "indirect" D_2-positive SPNs [46]. Furthermore, a
4 study by Ahmari et al, showed that hyperactivation of the OFC to DS pathway, increased self-
5 grooming in rats, which support our findings where lower OFC activity lead to lower self-
6 grooming [45].

7 *Nigro-striatal dopaminergic stimulation affects prepulse inhibition of the acoustic startle response*
8 *differently in males and females*

9 PPI is an autonomous behavioral response, which is highly modulated by components of the CSTC
10 circuit, in particular the PFC [47–50], striatum [51], and the SN [52]. Disruption of normal PPI is
11 evident in people with OCD [21,53]. Highly conserved across species, the PPI response serves as
12 a useful translational construct in brain research. While some dopamine agonists disrupt PPI when
13 given systemically, the relative contributions of D_1-and $D_{2/3}$ receptor pathways in this effect are
14 debated [54–57]. Thus, converging lines of clinical and preclinical evidence link the CSTC circuit,
15 dopamine, and PPI. The expression of PPI differs between rodent strains [58,59] and sex [60–62].
16 Indeed, we found that mDS-DREADD female rats had increased PPI at low prepulse amplitude
17 during chemogenetic activation, but males showed no such effect. Previous work showed that male
18 rats with SN lesions [52] as well as male mice with striatal lesions [63] displayed disruption of
19 PPI, but there was no corresponding investigation of female rats in those studies. In another
20 investigation, deep brain stimulation (DBS) of the NAc disrupted PPI in male WT rats, whereas
21 the same DBS rescued disrupted PPI in a male rat model of schizophrenia [49], which implies
22 context-dependence of the behavior consequences of stimulated dopamine release.
23
24 A limitation to this study lies in our use of CNO to activate DREADDs. CNO metabolizes *in vivo*
25 to clozapine, which is presumably the main agonist on DREADDs [23,64–66]. While clozapine is
26 an antagonist at endogenous dopamine $D_{2/3}$ and serotonin 5-HT_{2A} receptors, it has selectivity for
27 DREADDs when administered at the present low dose. Indeed, we did not observe any behavioural
28 effects of CNO/clozapine in control rats in this study, nor had we seen any occupancy at $D_{2/3}$ or 5-
29 HT_{2A} receptors in an earlier *in vivo* binding experiment [23]. Furthermore, clozapine treatment can
30 restore disrupted PPI [56,59,67], but neither we nor others [65] have measured any intrinsic effects
31 of CNO on PPI in WT or control animals at the dose used, which also argues for selective
32 activation of DREADDs.

33 *Nigro-striatal dopaminergic stimulation affects metabolic activity the medial prefrontal cortex and*
34 *orbitofrontal cortex.*

35 Metabolic mapping of [^{18}F]FDG uptake by PET can identify perturbation of neuronal circuits
36 related to behavior, chemical stimulation, or chemogenetic-induced circuit modulation [49,50,68–
37 71]. We found that chemogenetic activation in mDS-DREADD rats elicited hypometabolism in

10

1 fronto-cortical areas (Fig 4A and B). This confirms the behavioral findings described above
2 suggesting that mDS dopamine activation controls fronto-cortical neuronal activity though the
3 CSTC circuit. Serveas et al. showed that acute treatment of rats with the dopamine $D_{2/3}$ receptor
4 agonist quinpirole provoked a global increase in [18F]FDG whole-brain uptake, yet a relatively
5 lesser increase in NAc, mDS, and the fronto-cortical regions, i.e. mPFC, ACC and OFC [71],
6 suggesting a common mechanism to the present DREADD study. Globally increased [18F]FDG
7 uptake might hide regional differences in metabolism, emphasizing the importance of whole-brain
8 normalization between baseline and test conditions [72]. Our use of the human HRRT PET
9 scanner, which has lesser spatial resolution (2 mm) compared with contemporary dedicated small
10 animal scanners (1 mm), limits our ability to detect small focal changes in metabolism. We
11 accommodate the resolution issue by using relatively large bilateral VOIs.

12

13 *Nigro-striatal dopaminergic stimulation increase glutamate and N-acetylaspartylglutamic acid*
14 *in medial prefrontal cortex and glutamate levels in dorsal striatum.*

15 Our MR spectroscopy results showed increases in glutamate and NAAG in the mPFC, and
16 increased glutamate in the mDS during chemogenetic activation, which may seem at odds with the
17 PET finding of lower [18F]FDG uptake in frontal cortex. While the exact relationship between
18 [18F]FDG uptake and total glutamate levels is unknown, we suppose that glutamate is stored in the
19 terminals of glutamatergic afferents in the mPFC, which are presumably thalamic or cortical inputs
20 through the CSTC circuit, while NAAG is mainly located in interneurons [73]. Once released into
21 the synapse, glutamate is taken up by astroglial cells and converted into glutamine, whereas NAAG
22 is metabolized to NAA and glutamate [74,75]. In this scenario, the increased glutamate and NAAG
23 levels measured by MR spectroscopy during chemogenetic activation may thus reflect elevated
24 vesicular concentrations in thalamic or cortical afferent terminals, due to indirect inhibition via
25 mDS dopaminergic activation of the indirect (no-go) pathway. NAAG signaling is not completely
26 understood, but some evidence points towards it having an inhibitory effect on GABA release,
27 such that lower NAAG release might result in net inhibition of cortico-striatal projections [76].
28 Such an inhibition could account for the lower cortical [18F]FDG uptake and consequently lower
29 glutamatergic activity in the DS, resulting in increased vesicular glutamate content in DS.
30 Furthermore, we suppose that mDS-DREADD stimulation also stimulates dopamine neurons that
31 co-release glutamate [77,78], which in turn might favor the local astroglial conversion of glutamine
32 to glutamate [74,75].

33

34 As noted above, there is no general model to connect glutamate levels measured with MRS to
35 [18F]FDG uptake. One study reported no correlation between these two markers in WT mice,
36 although there was a clear inverse relationship in mGluR5 KO mice [79]. That finding resembles
37 present observations in the mDS-DREADD group, suggesting a similar perturbation of the
38 coupling between glutamate levels and energy metabolism. We did observe a change in DS
39 glutamate levels in the mCherry animals, as in our previous study, albeit at higher doses of CNO
40 [23]. Thus, it remains possible that CNO metabolism to clozapine may indeed contribute to the

11

1   cerebrometabolic changes reported in this study, albeit in the opposite direction; our results may

2   therefore underestimate the effect of mDS dopamine activity on local glutamate levels

3   *Translational relevance*

4   Changes in striatal dopamine and prefrontal cortical glutamate levels are held to be central

5   etiological factors for neuropsychiatric disorders that involve the CSTC circuit, such as OCD [13]

6   and Tourette's Syndrome [80]. In a recent PET study with DBS of the ventral striatum in people

7   with treatment-resistant OCD, increased dopamine release correlated with a decline in OCD

8   related symptoms [81]. Furthermore Nordstrom et al. found that systemic administration of the

9    $D_{2/3}$ receptor agonist bromocriptine suppressed "Tics" in a transgenic mouse model of Tourette's

10   Syndrome [82], supporting an earlier clinical report that bromocriptine may be helpful in some

11   OCD patients [83]. Our results are a step towards disentangling the functional and metabolic

12   effects of specific elements in the CSTC circuit and support the proposition that mDS might be a

13   relevant DBS target in neuropsychiatric diseases involving compulsive or impulsive behaviors.

14   *Conclusion*

15   We found that chemogenetic activation of dopamine neurons projecting to mDS potentiated rat

16   exploratory behavior, lowered self-grooming, and enhanced prepulse inhibition of the startle

17   response. These behavioral changes occurred in association with reduced metabolic activity in

18   frontal cortex as measured by [^{18}F]FDG PET and increased glutamate and NAAG levels in the

19   mPFC as measured by MRS. Our study thus revealed that dopamine signaling in mDS exerted

20   modulatory control of fronto-cortical metabolic activity and the orchestration of behavior related

21   to CSTC circuit function. These results support our hypothesis that dopamine release in the mDS

22   can be a driver for reduced cortical metabolism in distal parts of the CSTC circuit and suggest that

23   dopamine activation in the mDS reduce anxiety and compulsive behaviors.

24

12

Acknowledgments

Disclosures

Mikael Palner is collaborating with the pharmaceutical company Compass Pathways Plc (London, UK). All other authors declare no financial interests or potential conflicts of interest.

13

References

1. Peters SK, Dunlop K, Downar J. Cortico-striatal-thalamic loop circuits of the salience network: A central pathway in psychiatric disease and treatment. Front Syst Neurosci. 2016;10:1–23.

2. Ahmari SE, Dougherty DD. DISSECTING OCD CIRCUITS: FROM ANIMAL MODELS TO TARGETED TREATMENTS. Depress Anxiety. 2015;32:550–562.

3. Simpson EH, Kellendonk C. Insights About Striatal Circuit Function and Schizophrenia From a Mouse Model of Dopamine D2 Receptor Upregulation. Biol Psychiatry. 2017;81:21–30.

4. Howes OD, Kapur S. The Dopamine Hypothesis of Schizophrenia: Version III--The Final Common Pathway. Schizophr Bull. 2009;35:549–562.

5. Denys D, de Vries F, Cath D, Figee M, Vulink N, Veltman DJ, et al. Dopaminergic activity in Tourette syndrome and obsessive-compulsive disorder. Eur Neuropsychopharmacol. 2013;23:1423–1431.

6. Graybiel AM. Chapter 10 - The Basal Ganglia. Conn's Transl Neurosci. 2017:219–225.

7. Zuo C, Ma Y, Sun B, Peng S, Zhang H, Eidelberg D, et al. Metabolic imaging of bilateral anterior capsulotomy in refractory obsessive compulsive disorder: an FDG PET study. J Cereb Blood Flow Metab. 2013;33:880–887.

8. Horwitz B, Swedo SE, Grady CL, Pietrini P, Schapiro MB, Rapoport JL, et al. Cerebral metabolic pattern in obsessive-compulsive disorder: Altered intercorrelations between regional rates of glucose utilization. Psychiatry Res Neuroimaging. 1991;40:221–237.

9. Menzies L, Chamberlain SR, Laird AR, Thelen SM, Sahakian BJ, Bullmore ET. Integrating evidence from neuroimaging and neuropsychological studies of obsessive-compulsive disorder: the orbitofronto-striatal model revisited. Neurosci Biobehav Rev. 2008;32:525–549.

10. Whiteside SP, Port JD, Abramowitz JS. A meta–analysis of functional neuroimaging in obsessive–compulsive disorder. Psychiatry Res Neuroimaging. 2004;132:69–79.

11. Haber SN. Corticostriatal circuitry. Dialogues Clin Neurosci. 2016;18:7–21.

12. Aoki Y, Aoki A, Suwa H. Reduction of N-acetylaspartate in the medial prefrontal cortex correlated with symptom severity in obsessive-compulsive disorder: Meta-analyses of 1 H-MRS studies. Transl Psychiatry. 2012;2:e153-10.

13. Rosenberg DR, Macmaster FP, Keshavan MS, Fitzgerald KD, Stewart CM, Moore GJ. Decrease in caudate glutamatergic concentrations in pediatric obsessive-compulsive disorder patients taking paroxetine. J Am Acad Child Adolesc Psychiatry. 2000;39:1096–1103.

14. Rosenberg DR, Mirza Y, Russell A, Tang J, Smith JM, Banerjee SP, et al. Reduced anterior cingulate glutamatergic concentrations in childhood OCD and major depression versus healthy controls. J Am Acad Child Adolesc Psychiatry. 2004;43:1146–1153.

15. Palner M, Kjaerby C, Knudsen GM, Cumming P. Effects of unilateral 6-OHDA lesions on [3H]-N- propylnorapomorphine binding in striatum ex vivo and vulnerability to amphetamine-evoked dopamine release in rat. Neurochem Int. 2011;58:243–247.

16. Casteels C, Lauwers E, Bormans G, Baekelandt V, Van Laere K. Metabolic-dopaminergic mapping of the 6-hydroxydopamine rat model for Parkinson's disease. Eur J Nucl Med Mol Imaging. 2008;35:124–134.

17. Sala-Bayo J, Fiddian L, Nilsson SRO, Hervig ME, McKenzie C, Mareschi A, et al. Dorsal and ventral striatal dopamine D1 and D2 receptors differentially modulate distinct phases

14

of serial visual reversal learning. Neuropsychopharmacology. 2020;45:736–744.

18. Roughan J V., Flecknell PA. Behavioural effects of laparotomy and analgesic effects of ketoprofen and carprofen in rats. Pain. 2001;90:65–74.

19. Keller SH, L'Estrade EN, Dall B, Palner M, Herth M. Quantification accuracy of a new HRRT high throughput rat hotel using transmission-based attenuation correction: A phantom study. 2016 IEEE Nucl. Sci. Symp. Med. Imaging Conf. Room-Temperature Semicond. Detect. Work., IEEE; 2016. p. 1–3.

20. Hoenig K, Hochrein A, Quednow BB, Maier W, Wagner M. Impaired prepulse inhibition of acoustic startle in obsessive-compulsive disorder. Biol Psychiatry. 2005;57:1153–1158.

21. Ahmari SE, Risbrough VB, Geyer MA, Simpson HB. Impaired sensorimotor gating in unmedicated adults with obsessive-compulsive disorder. Neuropsychopharmacology. 2012;37:1216–1223.

22. Manning EE, Wang AY, Saikali LM, Winner AS, Ahmari SE. Disruption of prepulse inhibition is associated with compulsive behavior severity and nucleus accumbens dopamine receptor changes in Sapap3 knockout mice. Sci Rep. 2021;11:9442.

23. Baerentzen S, Casado-Sainz A, Lange D, Shalgunov V, Tejada IM, Xiong M, et al. The chemogenetic receptor ligand Clozapine N-oxide induces in vivo neuroreceptor occupancy and reduces striatal glutamate levels. Front Neurosci. 2019;13:187.

24. Armbruster BN, Li X, Pausch MH, Herlitze S, Roth BL. Evolving the lock to fit the key to create a family of G protein-coupled receptors potently activated by an inert ligand. Proc Natl Acad Sci U S A. 2007;104:5163–5168.

25. Witten IBB, Steinberg EEE, Lee SYY, Davidson TJJ, Zalocusky KAA, Brodsky M, et al. Recombinase-Driver Rat Lines: Tools, Techniques, and Optogenetic Application to Dopamine-Mediated Reinforcement. Neuron. 2011;72:721–733.

26. Salegio EA, Samaranch L, Kells AP, Mittermeyer G, San Sebastian W, Zhou S, et al. Axonal transport of adeno-associated viral vectors is serotype-dependent. Gene Ther. 2013;20:348–352.

27. Aschauer DF, Kreuz S, Rumpel S. Analysis of Transduction Efficiency, Tropism and Axonal Transport of AAV Serotypes 1, 2, 5, 6, 8 and 9 in the Mouse Brain. PLoS One. 2013;8:e76310.

28. San Sebastian W, Samaranch L, Heller G, Kells a P, Bringas J, Pivirotto P, et al. Adeno-associated virus type 6 is retrogradely transported in the non-human primate brain. Gene Ther. 2013;20:1178–1183.

29. Szablowski JO, Lee-gosselin A, Lue B, Malounda D, Shapiro MG. Non-Invasive Control of Neural Circuits. Nat Biomed Eng. 2018;2:1–11.

30. Mahler S V., Brodnik ZD, Cox BM, Buchta WC, Bentzley BS, Cope ZA, et al. Chemogenetic Manipulations of Ventral Tegmental Area Dopamine Neurons Reveal Multifaceted Roles in Cocaine Abuse. BioRxiv. 2018;39:503–518.

31. Cho J, Ryu S, Lee S, Kim J, Kim HI. Optimizing clozapine for chemogenetic neuromodulation of somatosensory cortex. Sci Rep. 2020;10:1–11.

32. Mimura K, Nagai Y, Inoue K, Matsumoto J, Hori Y, Sato C, et al. Chemogenetic activation of nigrostriatal dopamine neurons in freely moving common marmosets. 2021:1–10.

33. Sciolino NR, Plummer NW, Chen Y-W, Alexander GM, Robertson SD, Dudek SM, et al. Recombinase-Dependent Mouse Lines for Chemogenetic Activation of Genetically Defined Cell Types. Cell Rep. 2016;15:2563–2573.

34. Dell'Anno MT, Caiazzo M, Leo D, Dvoretskova E, Medrihan L, Colasante G, et al. Remote

15

control of induced dopaminergic neurons in parkinsonian rats. J Clin Invest. 2014;124:3215–3229.

35. Bonaventura J, Eldridge MAG, Hu F, Gomez JL, Sanchez-Soto M, Abramyan AM, et al. High-potency ligands for DREADD imaging and activation in rodents and monkeys. Nat Commun. 2019;10:4627.

36. Runegaard AH, Fitzpatrick CM, Woldbye DPD, Andreasen JT, Sørensen AT, Gether U. Modulating Dopamine Signaling and Behavior with Chemogenetics: Concepts, Progress, and Challenges. Pharmacol Rev. 2019;71:123–156.

37. Jackson BP, Dietz SM, Wightman RM. Fast-Scan Cyclic Voltammetry of 5-Hydroxytryptamine. Anal Chem. 1995;67:1115–1120.

38. Wang S, Tan Y, Zhang JE, Luo M. Pharmacogenetic activation of midbrain dopaminergic neurons induces hyperactivity. Neurosci Bull. 2013;29:517–524.

39. Boender AJ, de Jong JW, Boekhoudt L, Luijendijk MCM, van der Plasse G, Adan R a H. Combined use of the canine adenovirus-2 and DREADD-technology to activate specific neural pathways in vivo. PLoS One. 2014;9:e95392.

40. Prut L, Belzung C. The open field as a paradigm to measure the effects of drugs on anxiety-like behaviors: A review. Eur J Pharmacol. 2003;463:3–33.

41. Carli M, Prontera C, Samanin R. Effect of 5-HT1A agonists on stress-induced deficit in open field locomotor activity of rats: Evidence that this model identifies anxiolytic-like activity. Neuropharmacology. 1989;28:471–476.

42. Sturman O, Germain P, Bohacek J. Exploratory rearing : a context- and stress-sensitive behavior recorded in the open-field test. Stress. 2018;21:443–452.

43. Berridge KC, Aldridge JW. Super-stereotypy I: Enhancement of a complex movement sequence by systemic dopamine D1 agonists. Synapse. 2000;37:194–204.

44. Kalueff A V, Stewart AM, Song C, Berridge KC, Graybiel AM, Fentress JC. Neurobiology of rodent self-grooming and its value for translational neuroscience. Nat Rev Neurosci. 2016;17:45–59.

45. Ahmari SE, Spellman T, Douglass NL, Kheirbek MA, Simpson HB, Deisseroth K, et al. Repeated cortico-striatal stimulation generates persistent OCD-like behavior. Science. 2013;340:1234–1239.

46. Lu J, Cheng Y, Xie X, Woodson K, Bonifacio J, Disney E, et al. Whole-Brain Mapping of Direct Inputs to Dopamine D1 and D2 Receptor-Expressing Medium Spiny Neurons in the Posterior Dorsomedial Striatum. Eneuro. 2020:ENEURO.0348-20.2020.

47. Bubser M, Koch M. Prepulse inhibition of the acoustic startle response of rats is reduced by 6-hydroxydopamine lesions of the medial prefrontal cortex. Psychopharmacology (Berl). 1994;113:487–492.

48. Zavitsanou K. Dopamine Antagonists in the Orbital Prefrontal Cortex Reduce Prepulse Inhibition of the Acoustic Startle Reflex in the Rat. Pharmacol Biochem Behav. 1999;63:55–61.

49. Bikovsky L, Hadar R, Soto-Montenegro ML, Klein J, Weiner I, Desco M, et al. Deep brain stimulation improves behavior and modulates neural circuits in a rodent model of schizophrenia. Exp Neurol. 2016;283:142–150.

50. Rohleder C, Wiedermann D, Neumaier B, Drzezga A, Timmermann L, Graf R, et al. The Functional Networks of Prepulse Inhibition: Neuronal Connectivity Analysis Based on FDG-PET in Awake and Unrestrained Rats. Front Behav Neurosci. 2016;10:148.

51. Swerdlow NR, Geyer MA, Braff DL. Neural circuit regulation of prepulse inhibition of

16

startle in the rat: Current knowledge and future challenges. Psychopharmacology (Berl). 2001;156:194–215.

52. Koch M, Fendt M, Kretschmer BD. Role of the substantia nigra pars reticulata in sensorimotor gating, measured by prepulse inhibition of startle in rats. Behav Brain Res. 2000;117:153–162.

53. Ahmari SE, Risbrough VB, Geyer MA, Simpson HB. Prepulse Inhibition Deficits in Obsessive-Compulsive Disorder are More Pronounced in Females. Neuropsychopharmacology. 2016;41:2963–2964.

54. Rodrigues S, Salum C, Ferreira TL. Dorsal striatum D1-expressing neurons are involved with sensorimotor gating on prepulse inhibition test. J Psychopharmacol. 2017:026988111668687.

55. Bortolato M, Aru GN, Fà M, Frau R, Orrù M, Salis P, et al. Activation of D1, but not D2 receptors potentiates dizocilpine-mediated disruption of prepulse inhibition of the startle. Neuropsychopharmacology. 2005;30:561–574.

56. Geyer MA, Krebs-Thomson K, Braff DL, Swerdlow NR. Pharmacological studies of prepulse inhibition models of sensorimotor gating deficits in schizophrenia: A decade in review. vol. 156. 2001.

57. Weber M, Chang WL, Breier MR, Yang A, Millan MJ, Swerdlow NR. The effects of the dopamine D2 agonist sumanirole on prepulse inhibition in rats. Eur Neuropsychopharmacol. 2010;20:421–425.

58. Plappert CF, Pilz PKD, Schnitzler H-U. Factors governing prepulse inhibition and prepulse facilitation of the acoustic startle response in mice. Behav Brain Res. 2004;152:403–412.

59. Swerdlow, M.D., Ph.D. N. Discrepant Findings of Clozapine Effects on Prepulse Inhibition of Startle: Is It the Route or the Rat? Neuropsychopharmacology. 1998;18:50–56.

60. Faraday MM. Rat sex and strain differences in responses to stress. Physiol Behav. 2002;75:507–522.

61. Lehmann J, Pryce CR, Feldon J. Sex differences in the acoustic startle response and prepulse inhibition in Wistar rats. Behav Brain Res. 1999;104:113–117.

62. Tylš F, Páleníček T, Kadeřábek L, Lipski M, Kubešová A, Horáček J. Sex differences and serotonergic mechanisms in the behavioural effects of psilocin. Behav Pharmacol. 2016;27:309–320.

63. Baldan Ramsey LC, Xu M, Wood N, Pittenger C. Lesions of the dorsomedial striatum disrupt prepulse inhibition. Neuroscience. 2011;180:222–228.

64. Ilg A-K, Enkel T, Bartsch D, Bähner F. Behavioral Effects of Acute Systemic Low-Dose Clozapine in Wild-Type Rats: Implications for the Use of DREADDs in Behavioral Neuroscience. Front Behav Neurosci. 2018;12.

65. MacLaren DAA, Browne RW, Shaw JK, Radhakrishnan SK, Khare P, España RA, et al. Clozapine N-oxide administration produces behavioral effects in long-evans rats: Implications for designing DREADD experiments. ENeuro. 2016;3.

66. Gomez JL, Bonaventura J, Lesniak W, Mathews WB, Sysa-shah P, Rodriguez LA, et al. Chemogenetics Revealed: Dreadd Occupancy and Activation Via Converted Clozapine. Science (80-). 2017;357:503–507.

67. De Carolis L, Stasi MA, Serlupi-Crescenzi O, Borsini F, Nencini P. The effects of clozapine on quinpirole-induced non-regulatory drinking and prepulse inhibition disruption in rats. Psychopharmacology (Berl). 2010;212:105–115.

68. Apetz N, Kordys E, Simon M, Mang B, Aswendt M, Wiedermann D, et al. Effects of

17

subthalamic deep brain stimulation on striatal metabolic connectivity in a rat hemiparkinsonian model. DMM Dis Model Mech. 2019;12.

69. Urban DJ, Zhu H, Marcinkiewcz CA, Michaelides M, Oshibuchi H, Rhea D, et al. Elucidation of The Behavioral Program and Neuronal Network Encoded by Dorsal Raphe Serotonergic Neurons. Neuropsychopharmacology. 2015:1–12.

70. Michaelides M, Anderson SAR, Ananth M, Smirnov D, Thanos PK, Neumaier JF, et al. Whole-brain circuit dissection in free-moving animals reveals cell-specific mesocorticolimbic networks. J Clin Invest. 2013;123:5342–5350.

71. Servaes S, Glorie D, Verhaeghe J, Wyffels L, Stroobants S, Staelens S. [18F]-FDG PET neuroimaging in rats with quinpirole-induced checking behavior as a model for obsessive compulsive disorder. Psychiatry Res Neuroimaging. 2016;257:31–38.

72. Borghammer P, Cumming P, Aanerud J, Gjedde A. Artefactual subcortical hyperperfusion in PET studies normalized to global mean: Lessons from Parkinson's disease. Neuroimage. 2009;45:249–257.

73. Moffett JR, Namboodiri MAA, Neale JH. Enhanced carbodiimide fixation for immunohistochemistry: Application to the comparative distributions of N-acetylaspartylglutamate and N- acetylaspartate immunoreactivities in rat brain. J Histochem Cytochem. 1993;41:559–570.

74. Bak LK, Schousboe A, Waagepetersen HS. The glutamate/GABA-glutamine cycle: aspects of transport, neurotransmitter homeostasis and ammonia transfer. J Neurochem. 2006;98:641–653.

75. Agarwal N, Renshaw PF. Proton MR spectroscopy - Detectable major neurotransmitters of the brain: Biology and possible clinical applications. Am J Neuroradiol. 2012;33:595–602.

76. Zhao J, Ramadan E, Cappiello M, Wroblewska B, Bzdega T, Neale JH. NAAG inhibits KCl-induced [3H]-GABA release via mGluR3, cAMP, PKA and L-type calcium conductance. Eur J Neurosci. 2001;13:340–346.

77. Sulzer D, Joyce MP, Lin L, Geldwert D, Haber SN, Hattori T, et al. Dopamine neurons make glutamatergic synapses in vitro. J Neurosci. 1998;18:4588–4602.

78. Trudeau LÉ. Glutamate co-transmission as an emerging concept in monoamine neuron function. J Psychiatry Neurosci. 2004;29:296–310.

79. Joo YH, Kim YK, Choi IG, Kim HJ, Son YD, Kim HK, et al. In vivo glucose metabolism and glutamate levels in mGluR5 knockout mice: a multimodal neuroimaging study using [18F]FDG microPET and MRS. EJNMMI Res. 2020;10.

80. Wang Z, Maia T V, Marsh R, Colibazzi T, Gerber A, Peterson BS. The neural circuits that generate tics in Tourette's syndrome. Am J Psychiatry. 2011;168:1326–1337.

81. Figee M, Luigjes J, Smolders R, Valencia-Alfonso CE, Van Wingen G, De Kwaasteniet B, et al. Deep brain stimulation restores frontostriatal network activity in obsessive-compulsive disorder. Nat Neurosci. 2013;16:386–387.

82. Nordstrom EJ, Bittner KC, McGrath MJ, Parks CR, Burton FH. Hyperglutamatergic cortico-striato-thalamo-cortical circuit breaker drugs alleviate tics in a transgenic circuit model of Tourette's syndrome. Brain Res. 2015;1629:38–53.

83. Ceccherini-Nelli A, Guazzelli M. Treatment of refractory OCD with the dopamine agonist bromocriptine. J Clin Psychiatry. 1994;55:415–416.

Supplementary Materials

Study Design

18

1 Chemicals

2 Viral Vectors

3 Software

4 Breeding and Phenotypic Assessment in Animals

5 Immunohistochemistry details

6 Acoustic startle response

7 Prepulse inhibition of the acoustic startle response

8 [^{18}F]FDG PET scanning

9

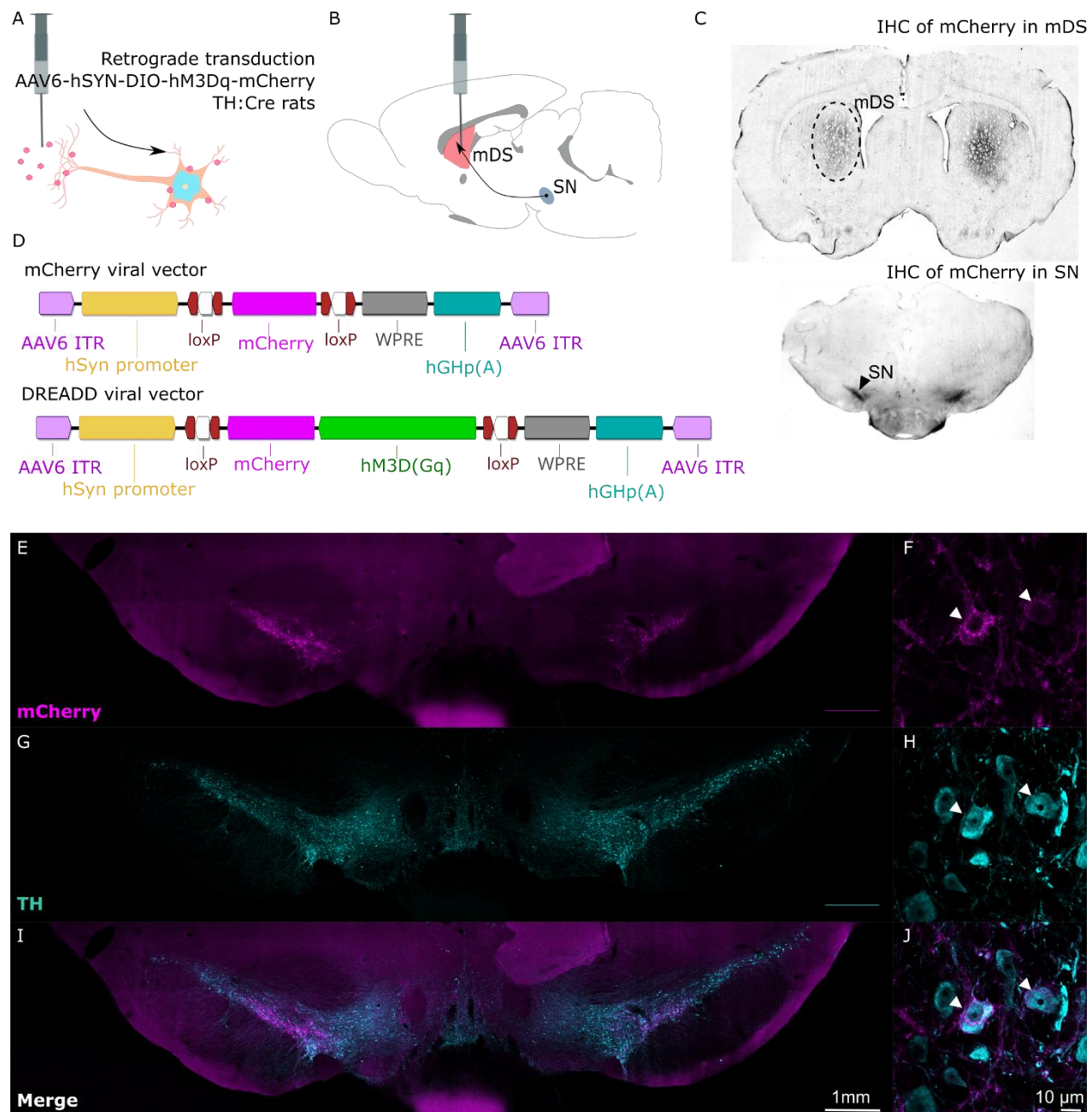10 ***Supplementary Figures***

16

19

1 **Figures**

2

3

4 Figure 1: A,B) Retrograde transduction of Cre-positive tyrosine hydroxylase (TH) expressing neurons in the
5 dorsomedial striatum. C) Immunohistochemical staining of mCherry in dorsomedial striatum and in substantia nigra.
6 D) Viral vectors used in the vehicle (mDS-mCherry) and chemogenetic (mDS-DREADD) transduction groups. E,G,I)
7 Fluorescent microscopy of mCherry (viral transducted) and TH-positive (dopamine) cells in the mesencephalon.
8 F,H,J) Magnifications of individual transducted cells (two examples labelled with white arrows) in the SN.
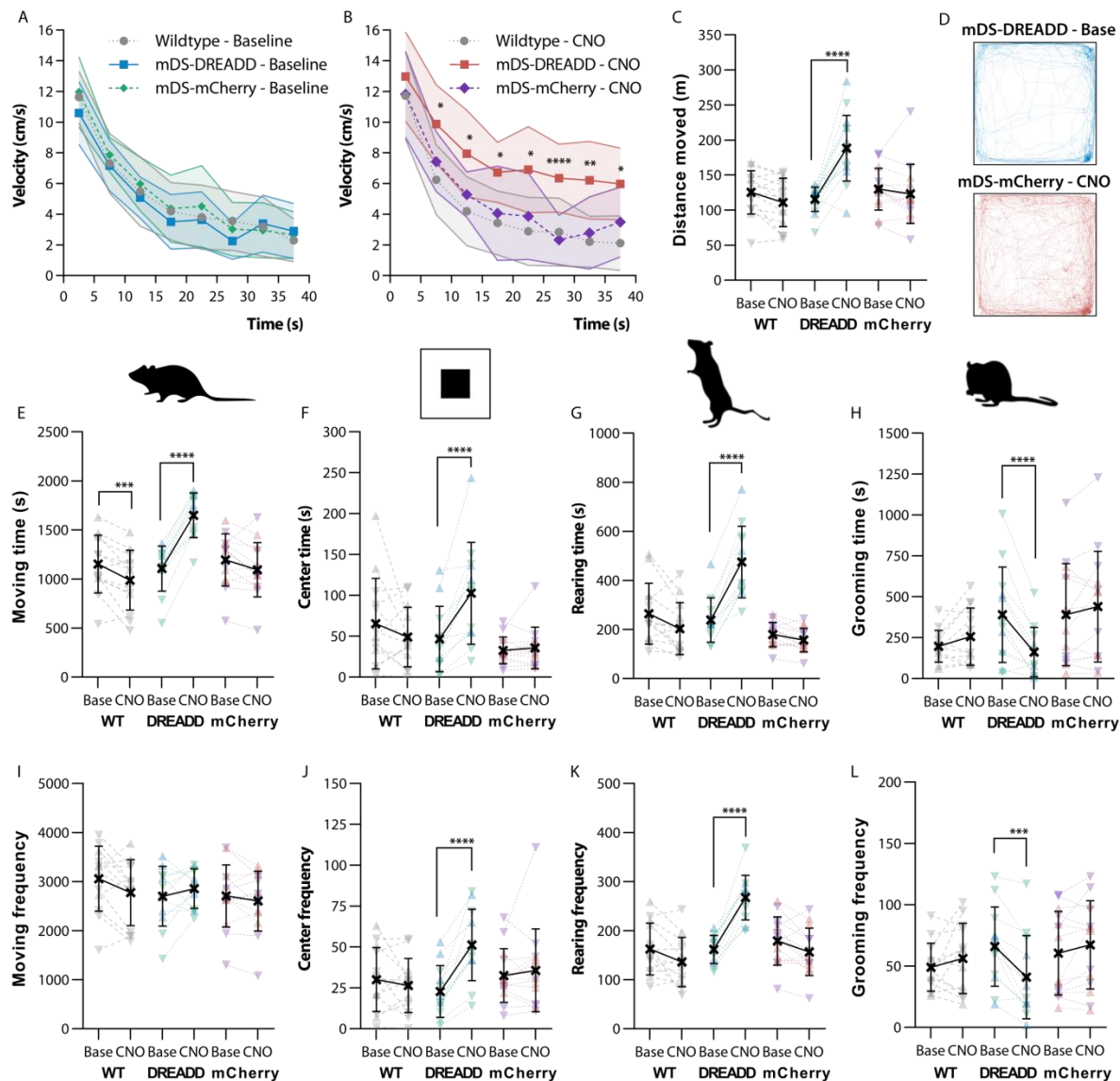
9

20

Figure 2: Open field behavior. A, B) Velocity over time in the open field. C) Total distance traveled over the whole-time course. D) Tracking of the median mDS-DREADD rat before and after CNO. E, F, G, H) Total time spent moving, in the center of the open field, rearing or grooming. I, J, K, L) Frequency of movement initiations, entries into the center square, rearings or grooming bouts. (♂ = ▲) (♀ = ▼).
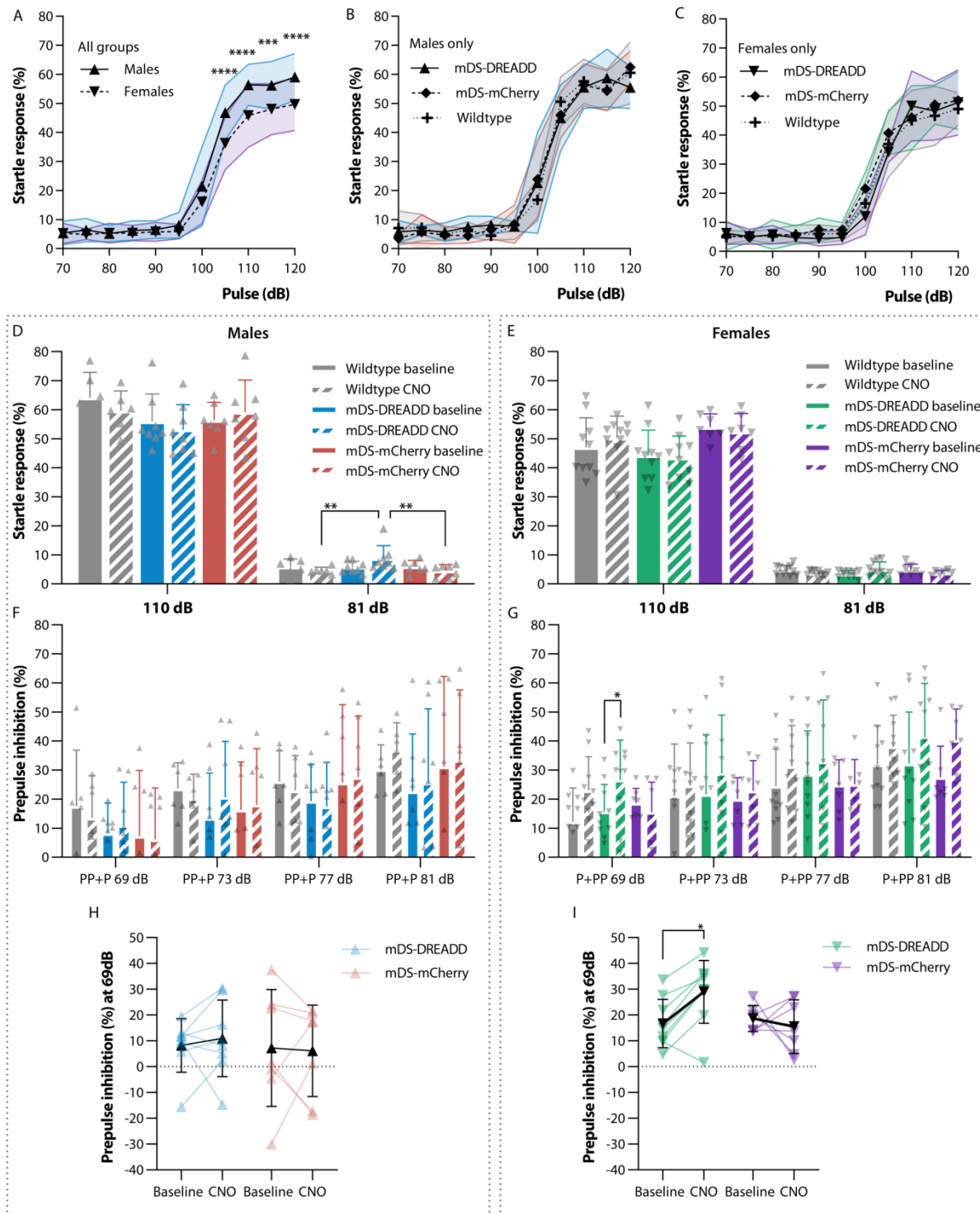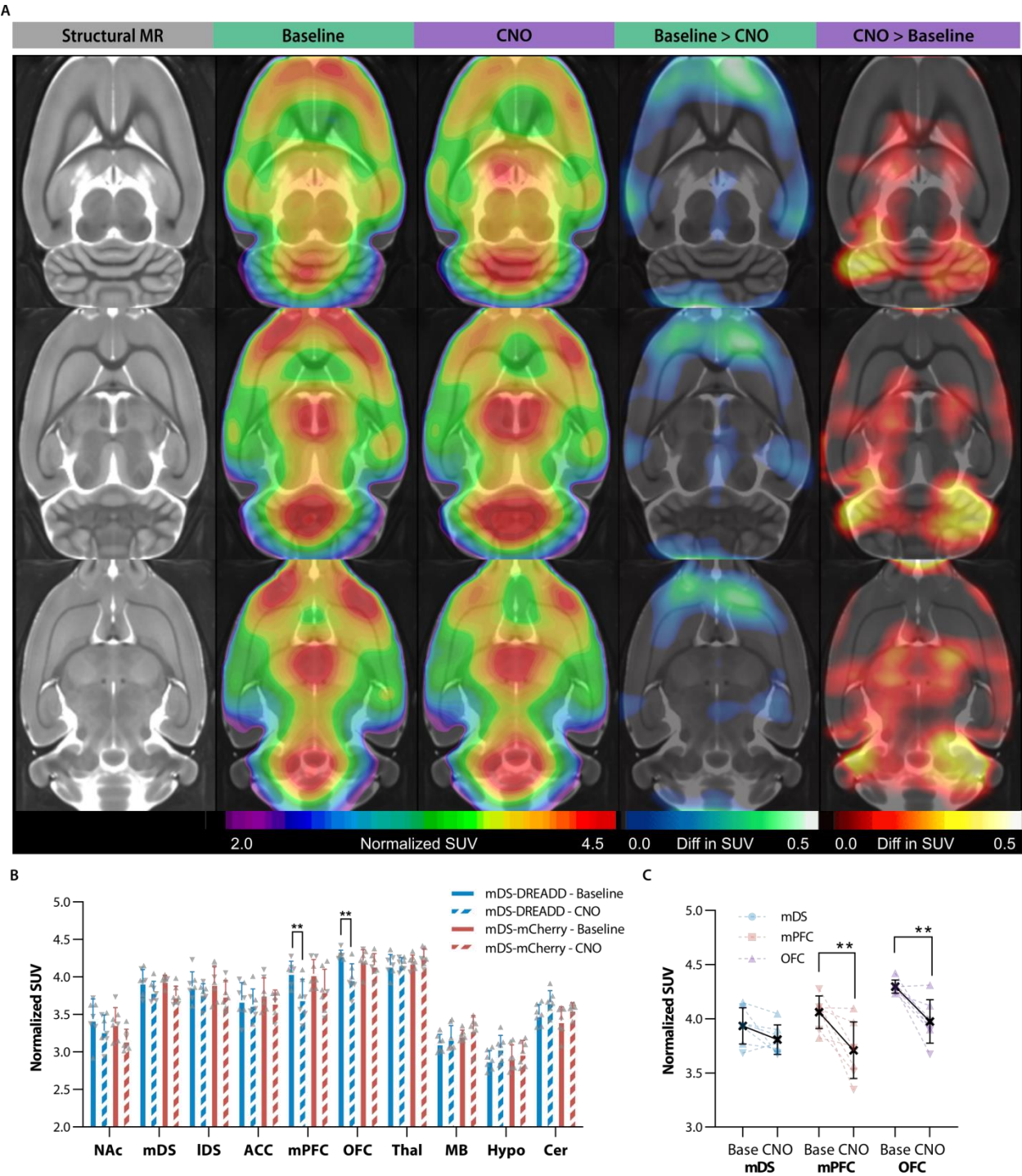
Figure 3: Acoustic startle response and prepulse inhibition. A, B, C) Startle response to various volumes of pulses. D, E) Startle response and effect of mDS-DREADD activation at high volume (110 dB) pulses and low volume (81 dB) prepulses. F, G) PPI as a result of prepulse intensities, negative PPI values are not shown in F and G to simplify the graph but were included in the statistical analysis. H, I) All PPI values at the lowest prepulse intensity (69 dB) pre and post CNO treatment to activate the nigro-striatal dopaminergic pathway. (♂ = ▲) (♀ =▼).

Figure 4: [18F]FDG images. A) [18F]FDG uptake in mDS-DREADD animal at baseline and after chemogenetic (CNO) stimulation (rainbow color), lower metabolic activity (blue color), higher metabolic activity (red color). B) Regional standard uptake values at all conditions and C) significant changes and individual animals in mDS, mPFC and OFC. (♂ = ▲) (♀ = ▼). Nucleus Acumbens (NAc), medial Dorsal Striatum (mDS), lateral Dorsal Striatum (lDS), Anterior Cingulate Cortex (ACC), medial Prefrontal Cortex (mPFC), Orbito Frontal Cortex (OFC), Thalamus (Thal), the midbrain including ventral tegmental area and substantia nigra (MB), Hypthalamus (Hyp) and Cerebellum (Cer).
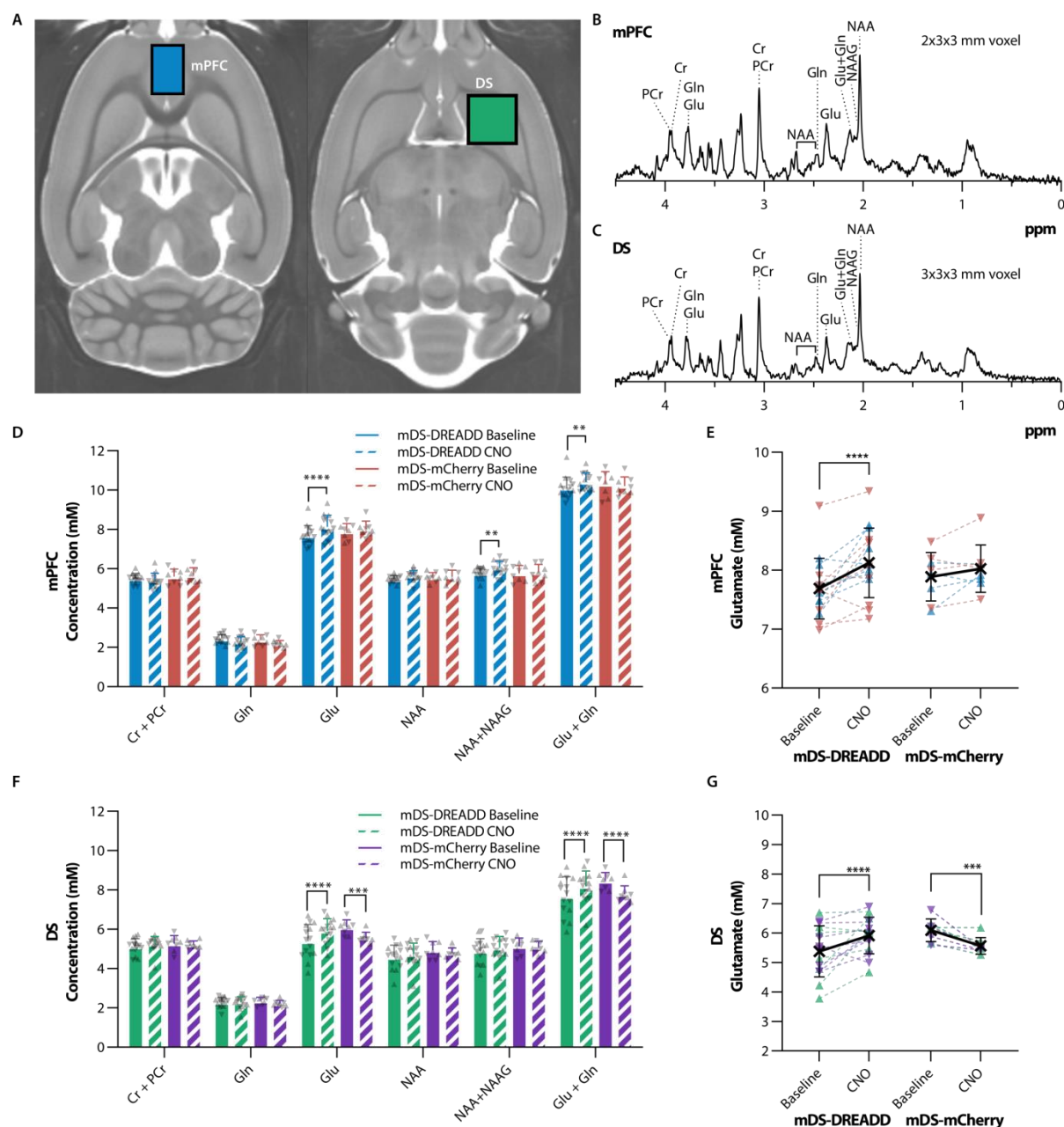
23

1

2
3 Figure 5: MR spectroscopy of neurochemicals in mDS-DREADD and mDS-mCherry animals. A) Voxel placement
4 in mPFC (blue voxel) and DS (green voxel). B,C) Sample spectra from the mPFC and DS. D,F) Neurochemical
5 concentrations in the mPFC in all conditions, E,G) significant changes in glutamate on the individual level. (♂ = ▲)
6 (♀ = ▼). Medial Prefrontal Cortex (mPFC), Dorsal Striatum (DS), Creatine (Cr), Phosphocreatine (PCr), Glutamine
7 (Gln), Glutamate (Glu), N-acetyl-aspartate (NAA) and N-acetyl-aspartatylglutamate (NAAG).